Computers and Structures 182 (2017) 526–539

Contents lists available at ScienceDirect

Computers and Structures

journal homepage: www.elsevier.com/locate/compstruc

The finite element method with overlapping elements – A new paradigm for CAD driven simulations ☆

Klaus-Jürgen Bathe *, Lingbo Zhang

Massachusetts Institute of Technology, Cambridge, MA 02139, USA

ARTICLE INFO

Article history:
Received 4 August 2016
Accepted 24 October 2016
Available online 26 January 2017

Keywords:
Finite elements
Meshless methods
Overlapping elements
Meshing
CAD
Geometry clean-up

ABSTRACT

A major difficulty in finite element analysis is the preparation of an effective mesh leading to a good response solution. In engineering analyses of complex components, oftentimes, much more time is spent to arrive at an adequate mesh than to obtain the solution of the established finite element model. The difficulty in meshing is due to the fact that finite elements need to abut each other and cannot overlap. This can lead to highly distorted elements, e.g. sliver elements, reducing the accuracy of solution. In practice, to establish an effective mesh, frequently, significant expertise in building meshes is needed, because great care must be taken in cleaning up the CAD geometry and preparing an effective mesh.

The objective in this paper is to present a new finite element solution scheme including meshing in which the elements can overlap. The property that finite elements can overlap removes many of the meshing difficulties, leads to an effective meshing procedure and an overall easy-to-use solution scheme for an analyst or a designer.

We first present the meshing scheme that we propose, which combines the use of traditional finite elements and overlapping finite elements. A particular feature is that the meshing procedure can be directly embedded in CAD driven solutions. We then present the theory used for the formulation of the overlapping finite elements and the coupling with traditional finite elements. We consider spherical and brick-shaped overlapping finite elements for which the theory is largely based on the formulation of the method of finite spheres. Finally, we illustrate the complete solution scheme in the analysis of some two-dimensional problems using the CAD geometry as the starting point.

While the paper presents a new paradigm for analysis in CAD environments, with much potential, we realize that much further study and research is needed on some of the important ingredients of the method to render the complete procedure effective for general practical engineering analyses of static and dynamic problems.

1. Introduction

The finite element method is now established as an effective procedure to simulate on the computer the behavior of structures. Quite general structures can be analyzed, from large scale to very small scale structures, such as from large bridges, to motor cars, to DNA structures [1,2]. However, in all finite element simulations, it is necessary to establish an appropriate and effective mesh of elements, which may require a large effort for the analyst. Since also experience is needed to construct an adequate mesh, we see that mostly only experienced analysts can perform an effective simulation, even in linear analysis. The difficulties of obtaining an adequate and hence good mesh should ideally be removed from the analysis process. If this is achieved, the finite element method will be much more employed, notably by designers in the CAD environment.

Since there are the difficulties of meshing, many meshless methods have been designed, see Refs. [3–9] and the references therein. Much research effort has been expended to develop an effective meshless method. Nevertheless, all reliable meshless methods (that do not entail the adjustment of numerical factors [1]) have been shown to be numerically expensive for practical usage when compared with the traditional finite element method [10–15] and, while the overall aim of using meshless methods is very attractive, such methods have not yet found broad use in engineering practice.

☆ This paper is an enlargement of the paper presented by KJ Bathe at the SEMC 2016 Conference, University of Cape Town, South Africa, Sept. 2016.

* Corresponding author.
E-mail address: kjb@mit.edu (K.J. Bathe).

http://dx.doi.org/10.1016/j.compstruc.2016.10.020
0045-7949/

The objective in this paper is to present a solution scheme that uses largely traditional finite elements in uniform mesh layouts in the interior of the analysis domain and overlapping finite elements near the boundaries to cover the complete analysis domain. The primary aim is to reduce the time and effort spent on meshing.

An approach using "overlapping grids" in finite difference solutions (the Chimera approach) has been developed and used for some time in fluid dynamics, see Refs. [16–20]. Here finite difference grids are superimposed at their boundaries to cover the complete analysis domain. Our approach is related to those schemes but with the important distinction that we use finite elements and overlapping finite elements with much more generality in direct coupling to CAD geometries for meshing complex geometries.

We first present the meshing scheme with some emphasis on how it can be used effectively in CAD driven analyses. Then we summarize the theory of the overlapping finite elements, which can be spherical and brick-shaped elements, including how the coupling to traditional elements is reached.

To indicate the accuracy obtained and resulting computational expense when only using overlapping finite elements, we consider briefly the method of finite spheres without traditional finite elements [21–23]. This discussion shows the potential of using overlapping finite elements.

Next we illustrate the complete analysis procedure based on the new proposed meshing scheme in the solution of some two-dimensional problems. The response is reached by automatically discretizing the surface (boundary) of the CAD part, automatic meshing and the solution. This illustration shows the potential of the complete analysis approach.

The paper is expanding on ideas presented earlier in Ref. [24] (from which some text is used) giving new theoretical details and results. We present a new analysis paradigm, the general theory, and results of some simple analysis problems. However, as concluded in the paper, considerable research and development effort is still needed to study and further develop the meshing and analysis scheme in order to fully harvest the potential of the new approach.

2. An effective way of meshing using traditional and overlapping finite elements

Considering the requirements of a reliable and generally applicable analysis procedure [1], the method of finite spheres can be regarded as one of the most effective meshless methods available. Like all meshless methods, it was designed to reduce the time of preparing a numerical model for a given physical problem, namely, the time and effort spend on meshing. However, while having some good attributes, the method is in most cases numerically too expensive to use.

Our objective in this section is to propose that overlapping elements – the spheres in the method of finite spheres being one type of such elements – be used effectively with very simple Cartesian meshes of traditional finite elements.

To explain the novel approach of using overlapping finite elements, consider the geometry of a two-dimensional part generated using a CAD software, like SolidWorks, as shown in Fig. 1. The discretization would be performed as follows.

The first step is to generate a two-dimensional grid over the whole part, with Δx and Δy as distances between the lines, see Fig. 2(a). An algorithm would automatically calculate the spacing depending on the geometry, or the analyst would specify the spacing. The part can now be thought of as being 'immersed' in a grid, which can obviously be established with negligible human and computational effort.

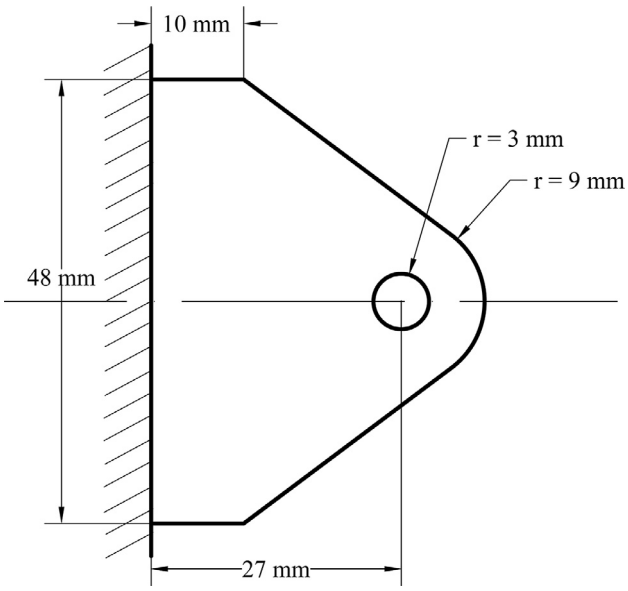

Fig. 1. A typical CAD part analyzed.

The second step is that "straight line segments" Δs are used for discretizing the boundary of the part. This segment length is best established automatically by an algorithm using the geometry of the CAD part and in general will vary in size along the boundary. Here, Δs should be small enough so that the segment lines will represent the complete boundary of the part with sufficient accuracy, see Fig. 2(b).

However, the segment length Δs can also be such that small imperfections in the CAD geometry, resulting from the complexities of the boundary representation using CAD procedures, are ignored and not included in the analysis. Some such cases leading to a non-watertight geometry are shown in Fig. 3. An important ingredient in the scheme is that Δs can vary along the boundary and can be selected automatically to discretize the boundary ignoring imperfections.

The third step is that all Cartesian cells that do not cut the numerical boundary established in step 2 are represented by traditional finite elements, like 4-node elements. The other cells are removed, see Fig. 2(c), and hence some empty space is generated.

The fourth step is that the boundary is meshed with overlapping finite elements using the segment length as spacing. It is important to place the centers of these elements at the boundary points (the end points of the boundary segment lines) because then the displacement boundary conditions can be easily imposed [7,22]. These overlapping finite elements must extend over to the traditional finite elements (established in step 3) to fill in all empty space and provide for the coupling of the traditional and overlapping elements. If the one layer of spheres placed along the boundary does not sufficiently extend into the traditional finite elements, additional overlapping elements are placed. We illustrate this process generically in Fig. 2(d).

In three-dimensional analysis, the same steps are followed but the grid is for the three Cartesian coordinate directions and triangular surfaces of varying size are used to discretize the surface boundary of the CAD part in step 2. Then traditional brick finite elements are employed in conjunction with overlapping brick or spherical elements.

The coupling between the overlapping finite elements and the traditional finite elements is achieved as presented in Section 3.2.

The effort in meshing using this approach is much smaller than using traditional finite elements throughout the analysis domain.

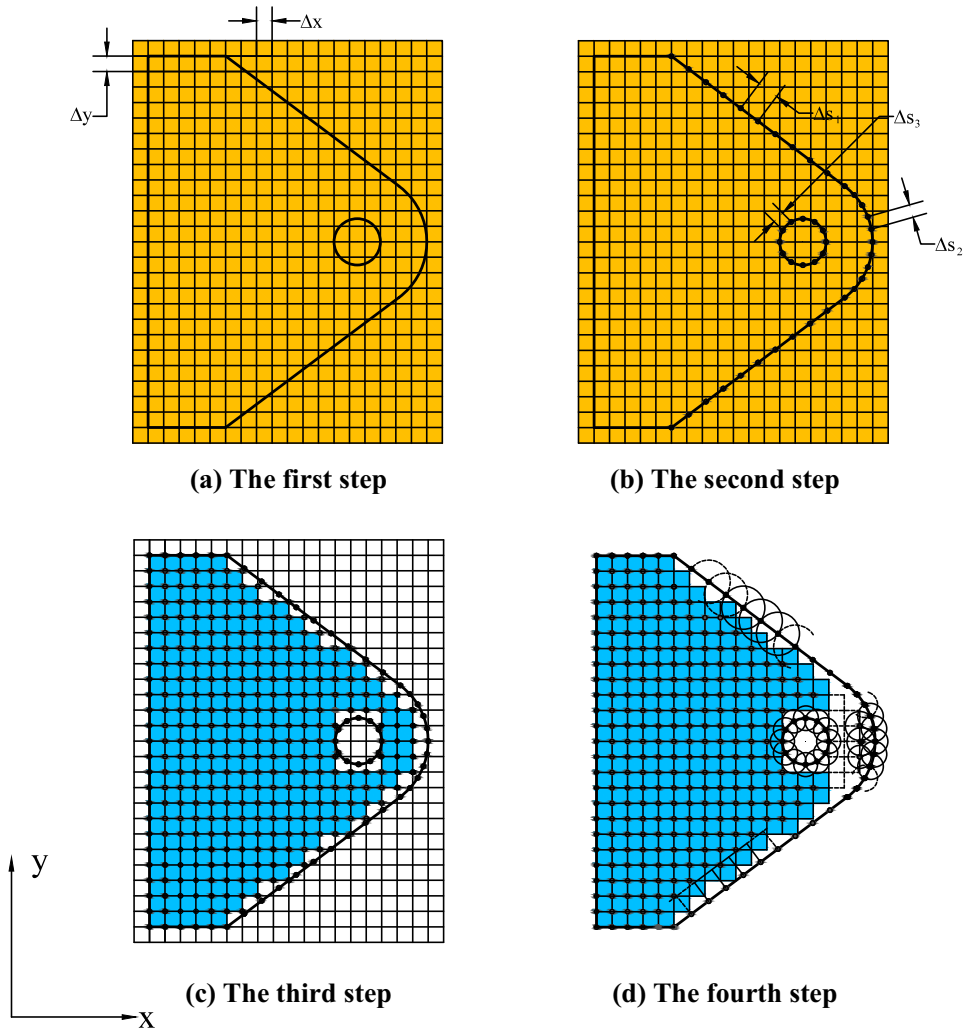

Fig. 2. The typical CAD part as generically discretized; the generated $(\Delta x, \Delta y)$ grid; the straight line Δs-segmentation of the boundary; the internal cells retained and converted to 4-node traditional finite elements; some overlapping disks, quadrilateral elements used along and near the boundary; note that some internal cells of step 3 have been turned into overlapping elements in step 4.

The accuracy of solution for a given number of elements is in many analyses probably increased because mostly undistorted elements are used. The computational time might be in most cases larger than when using the traditional finite element discretizations. However, this new approach will quite likely require much less total time for an analysis (time of meshing by an engineer + computer solution time of the finite element model), with of course the actual time gained dependent on the specific analysis performed.

In the above presentation we assumed that the objective is to largely use traditional finite elements, and reduce the time required for meshing. Hence the overlapping finite elements are only used on and near the boundary of the domain. However, the use of the overlapping finite elements can also be attractive to refine a mesh, and to embed special functions in the approximation space like "crack capturing" functions for the solution of stresses near crack tips, or harmonic functions for wave propagation problems, see e.g. Refs. [21,25].

3. The overlapping finite elements

The objective in this section is to present the theoretical formulation of the overlapping finite elements including the coupling between these and traditional elements, the numerical integration used for the element matrices, and, briefly, some analysis experiences when only the overlapping (spherical) finite elements are used.

3.1. The theory of overlapping elements

As an example for exposition of the theory, consider the body shown in Fig. 4 discretized using spheres. For illustrative purposes we show in fact disks as used in two-dimensional solutions, but in three-dimensional analysis, there would be spheres. In this analysis case, we only use overlapping finite elements. As indicated, the spheres overlap each other, overlap the boundary of the body, and together cover the complete body.

In a traditional finite element mesh, the elements need to abut each other and must not overlap, also not the boundary of the analysis domain. Hence the only difference in the discretization used in Fig. 4, is that the overlapping is present.

Using the general principle of virtual work, as in traditional finite element analysis, we have

Find $\mathbf{u} \in H^1(\Omega)$ such that

$$\int_\Omega \boldsymbol{\varepsilon}^{\mathrm{T}}(\mathbf{v})\mathbf{C}\boldsymbol{\varepsilon}(\mathbf{u})\mathrm{d}\Omega = \int_\Omega \mathbf{v}^{\mathrm{T}}\mathbf{f}^B d\Omega + \int_{S_f} \mathbf{v}^{\mathrm{T}}\mathbf{f}^S \mathrm{d}S + \int_{S_u} \bar{\boldsymbol{\lambda}}^{\mathrm{T}}(\mathbf{u}-\mathbf{u}^S)\mathrm{d}S + \int_{S_u} \boldsymbol{\lambda}^{\mathrm{T}}\mathbf{v}\,\mathrm{d}S \quad \forall \mathbf{v} \in H^1(\Omega) \tag{1}$$

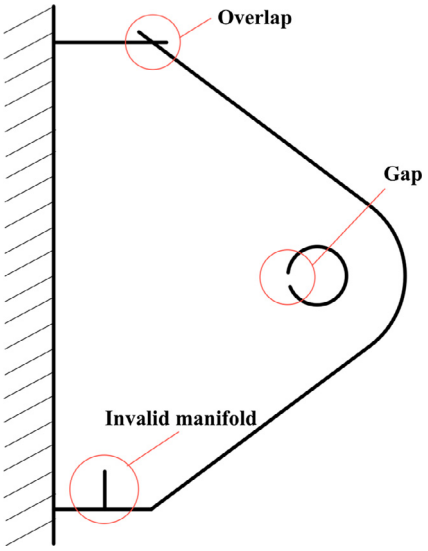

Fig. 3. Schematic of three imperfections in the CAD representation by non-uniform rational B-splines. The three imperfections are automatically ignored in the discretization of the CAD boundary.

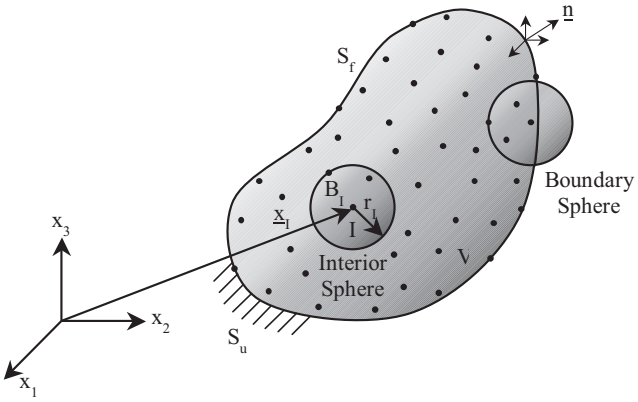

Fig. 4. General problem domain V with domain boundary $S = S_u \cup S_f$.

where $\mathbf{u}$ is the unknown displacement field, $\boldsymbol{\varepsilon}$ is the strain vector, $\mathbf{C}$ is the elasticity matrix, $\mathbf{v}$ is the virtual displacement field, $\mathbf{f}^S$ is the prescribed surface traction vector on the boundary S_f, $\mathbf{u}^S$ is the prescribed displacement vector on the boundary S_u, $\mathbf{f}^B$ is the applied body force vector and H^1 is the first order Hilbert space. The last two terms are Lagrange multiplier terms that impose the displacement boundary condition with

$$\boldsymbol{\lambda} = \mathbf{NC}\boldsymbol{\varepsilon}(\mathbf{u}), \quad \bar{\boldsymbol{\lambda}} = \mathbf{NC}\boldsymbol{\varepsilon}(\mathbf{v}) \tag{2}$$

and the direction matrix $\mathbf{N}$, in two-dimensional analysis

$$\mathbf{N} = \begin{bmatrix} n_x & 0 & n_y \\ 0 & n_y & n_x \end{bmatrix}$$

The overbar signifies a virtual quantity. We note that these terms furnish a symmetric contribution to the stiffness matrix because $\boldsymbol{\varepsilon}$ is a function of $\mathbf{u}$.

There might be the question of why these two terms furnish a negative contribution to the stiffness matrix, since the imposition of the displacement boundary conditions might also be achieved using ($\mathbf{u}^s$-$\mathbf{u}$) instead of ($\mathbf{u}$-$\mathbf{u}^s$) with the Lagrange multiplier. However, if we start with the general principle of virtual work expression for actions on the boundary S_u, those accounting for the right-hand side of the governing equation (1), and transform in the usual way by chain differentiation, we directly obtain the Lagrange multiplier terms with the signs given in Eq. (1) [7]. Hence this formulation is consistent with the differential formulation of the continuum problem.

Substituting from Eq. (2) into Eq. (1), we obtain

$$\int_\Omega \boldsymbol{\varepsilon}^{\mathrm{T}}(\mathbf{v})\mathbf{C}\boldsymbol{\varepsilon}(\mathbf{u})\mathrm{d}\Omega - \int_{S_u}\left[\boldsymbol{\varepsilon}^{\mathrm{T}}(\mathbf{v})\mathbf{C}\mathbf{N}^{\mathrm{T}}\mathbf{u} + \mathbf{v}^{\mathrm{T}}\mathbf{N}\mathbf{C}\boldsymbol{\varepsilon}(\mathbf{u})\right]\mathrm{d}S = \int_\Omega \mathbf{v}^{\mathrm{T}}\mathbf{f}^B d\Omega + \int_{S_f}\mathbf{v}^{\mathrm{T}}\mathbf{f}^S\mathrm{d}S - \int_{S_u}\boldsymbol{\varepsilon}^{\mathrm{T}}(\mathbf{v})\mathbf{C}\mathbf{N}^{\mathrm{T}}\mathbf{u}^S\,\mathrm{d}S, \quad \forall\mathbf{v}\in H^1(\Omega) \tag{3}$$

We note that in this equation, the only unknown is the displacement field $\mathbf{u}$, which we interpolate using for a component u

$$u = \sum_{j=1}^{N}\sum_{n\in\mathfrak{I}} h_{jn}\alpha_{jn}^u \tag{4}$$

where N is the number of overlapping finite elements

$$h_{jn} = \varphi_j p_n \tag{5}$$

and

$$\varphi_j = \frac{W_j}{\sum_{i=1}^{N} W_i} \tag{6}$$

with p_n denoting the nth polynomial term from

$$\mathbf{p}^T = [1 \quad x \quad y \quad xy \quad \ldots] \tag{7}$$

which defines $\mathfrak{I}$. Note that we can include in $\mathbf{p}$ only a few basic terms, also higher order terms, and special functions.

The weight function, referred to as Shepard function, in Eq. (6) is defined differently for the different shapes of overlapping elements. Consider the disk and square elements shown in Fig. 5.

We have for the disk of unit radius

$$W_j = 1 - 6s^2 + 8s^3 - 3s^4 \tag{8}$$

where s is the distance from the center of the disk. For the square of side-length 2, we have

$$W_j = W_{jx} \times W_{jy} \tag{9}$$

where

$$W_{jx} = 1 - 6x^2 + 8x^3 - 3x^4 \tag{10}$$

$$W_{jy} = 1 - 6y^2 + 8y^3 - 3y^4 \tag{11}$$

Eqs. (8)–(11) can of course directly be generalized to a disk of different radius than unity and a general quadrilateral element using isoparametric coordinates [1].

The solution unknowns are defined at the centers of the overlapping finite elements so that we obtain the governing equations with the usual procedures in finite element analysis

$$\mathbf{M}\ddot{\boldsymbol{\alpha}} + \mathbf{K}\boldsymbol{\alpha} = \mathbf{R} \tag{12}$$

where the vector of unknown solution variables is

$$\boldsymbol{\alpha}^{\mathrm{T}} = [\boldsymbol{\alpha}_{11} \quad \boldsymbol{\alpha}_{12} \quad \ldots \quad \boldsymbol{\alpha}_{21} \quad \boldsymbol{\alpha}_{22} \quad \ldots \quad \boldsymbol{\alpha}_{N1} \quad \boldsymbol{\alpha}_{N2} \quad \ldots \quad \boldsymbol{\alpha}_{Nm}] \tag{13}$$

with $\boldsymbol{\alpha}_{ij} = [\alpha_{ij}^u \ \alpha_{ij}^v]$ and m the number of terms included in $\mathbf{p}$. In Eq. (12), we use the usual notation of finite element analysis, $\mathbf{K}$ is the stiffness matrix, $\mathbf{M}$ is the mass matrix and a dot denotes time derivative. Damping effects could be included as usual [1]. The expressions for $\mathbf{K}$, $\mathbf{M}$ and $\mathbf{R}$ are for node I and degree of freedom m of the form [7,25]

$$\sum_{J=1}^{N}\sum_{n\in\mathfrak{I}}\mathbf{M}_{ImJn}\ddot{\boldsymbol{\alpha}}_{Jn} + \sum_{J=1}^{N}\sum_{n\in\mathfrak{I}}\mathbf{K}_{ImJn}\boldsymbol{\alpha}_{Jn} = \mathbf{f}_{Im} + \hat{\mathbf{f}}_{Im} \tag{14}$$

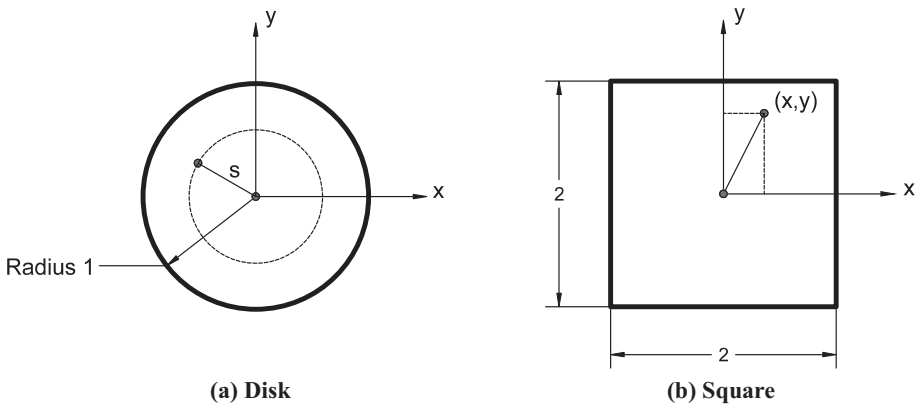

Fig. 5. Schematic of two shapes of overlapping elements.

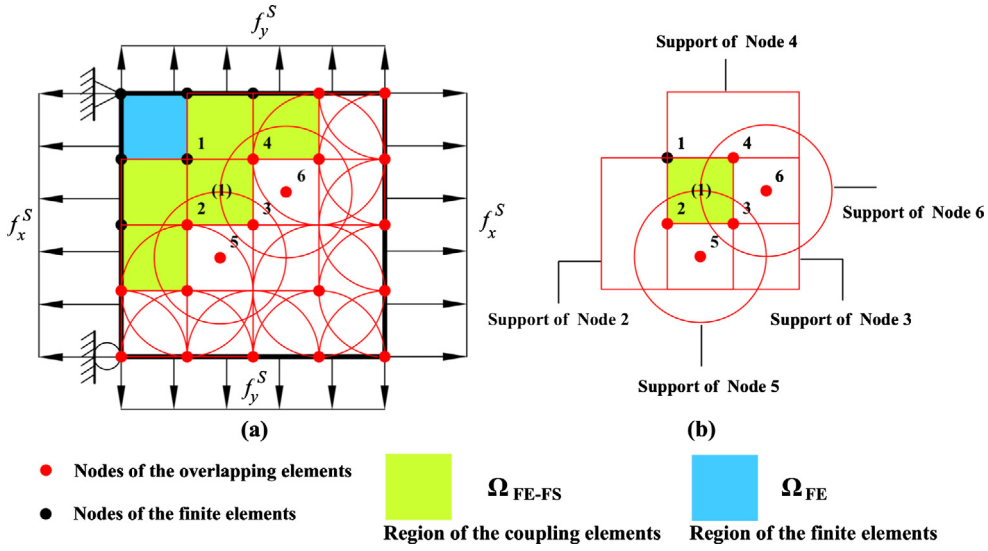

Fig. 6. Patch test study of the new scheme in plane strain conditions. (a) Mesh of the new scheme and (b) supports of the overlapping elements that intersect the coupling element 1.

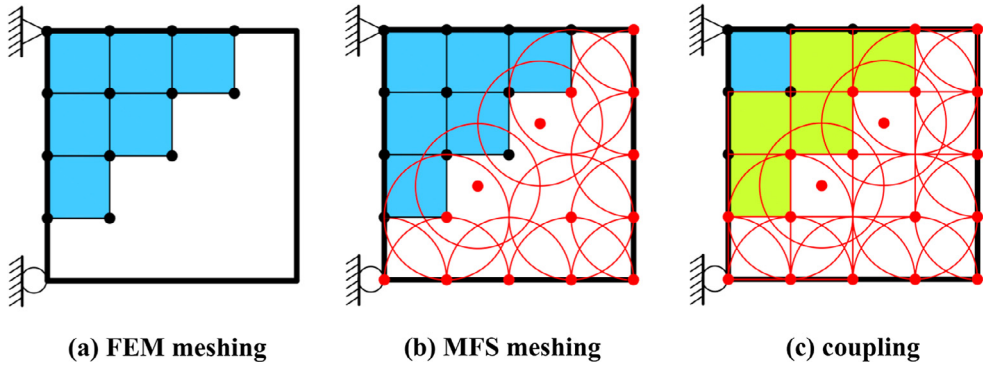

Fig. 7. Application of the new coupling scheme. 4-node finite elements are generated; the overlapping elements are used and extended to the region of finite elements; nodes at the coupling boundary are replaced by overlapping element nodes; finite elements adjacent to the coupling boundary become the coupling elements.

where the mass matrix is

$$\mathbf{M}_{ImJn} = \int_{V_I} \mathbf{H}_{Im} \rho \mathbf{H}_{Jn} \mathrm{d}V \tag{15}$$

the stiffness matrix is

$$\mathbf{K}_{ImJn} = \int_{V_I} \mathbf{B}_{Im}^{\mathrm{T}} \mathbf{C} \mathbf{B}_{Jn} \mathrm{d}V \tag{16}$$

and the body force load vector is

$$\mathbf{f}_{Im} = \int_{V_I} \mathbf{H}_{Im} \mathbf{f}^B \mathrm{d}V \tag{17}$$

with $V_I = V \cap B(\mathbf{x}_I, r_I)$.

The traction force vector corresponding to node I and degree of freedom m is

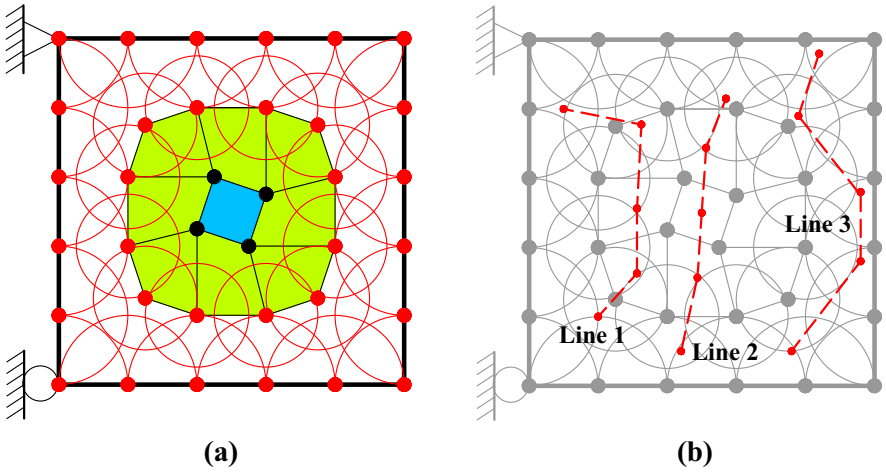

Fig. 8. Patch test study of the new scheme with distorted finite elements in plane strain conditions (thickness = 1.0, $E = 100$, $\nu = 0.3$), (a) mesh of the new scheme and (b) lines through elements for stress evaluation.

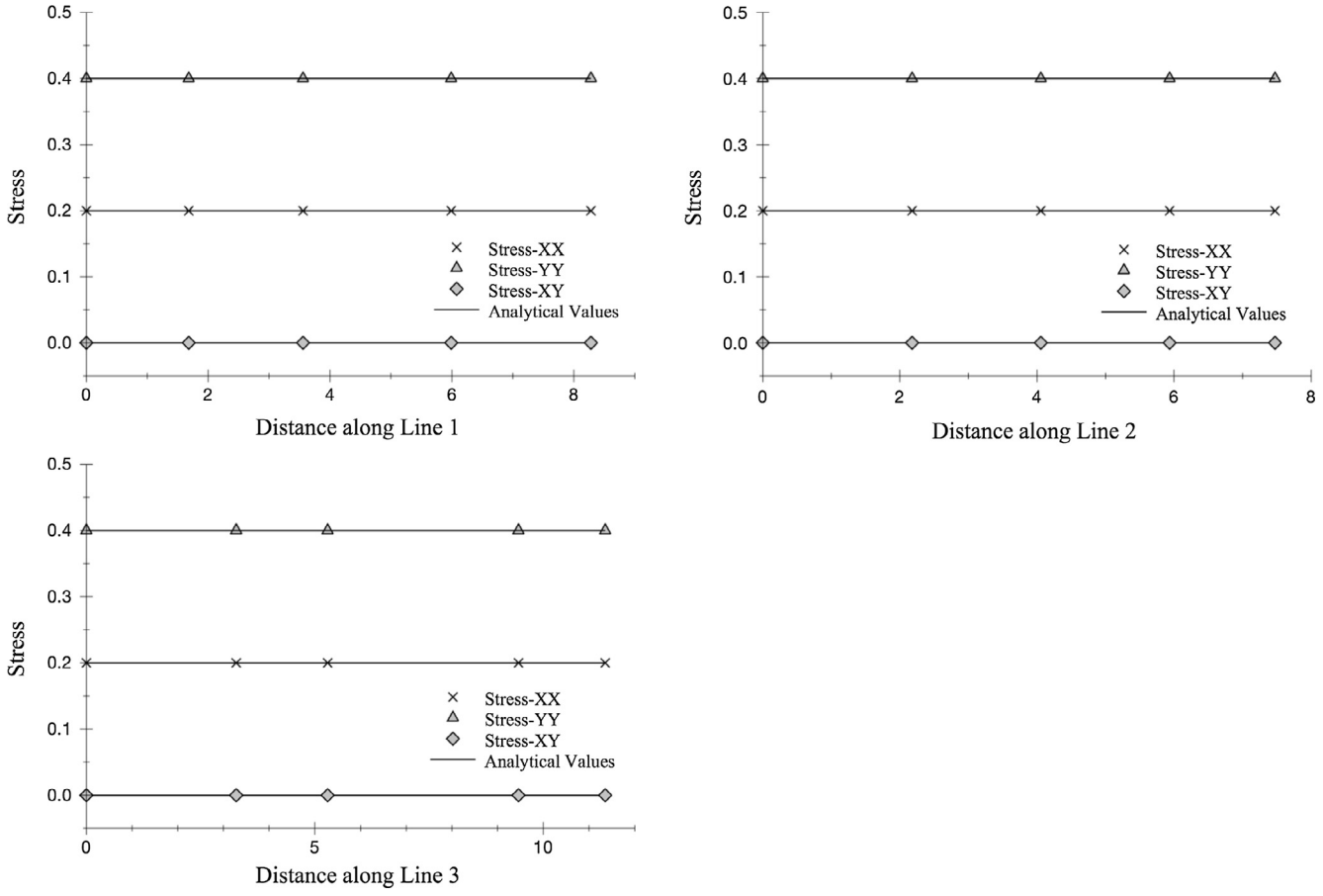

Fig. 9. Calculated stresses in the patch test study of Fig. 8 when constant normal stresses ($\tau_{xx} = 0.2$ and $\tau_{yy} = 0.4$) are applied on the boundary.

$$\hat{\mathbf{f}}_{Im} = \begin{cases} \mathbf{0}, & \text{for an interior sphere} \\ \int_{S_{f_I}} \mathbf{H}_{Im}\mathbf{f}^S \mathrm{d}S, & \text{for a Neumann boundary sphere} \\ \sum_{J=1}^{N}\sum_{n\in\Im} \mathbf{KU}_{ImJn}\boldsymbol{\alpha}_{Jn} - \mathbf{fU}_{Im}, & \text{for a Dirichlet boundary sphere} \end{cases} \tag{18}$$

where

$$\mathbf{KU}_{ImJn} = \int_{S_{u_I}} \mathbf{H}_{Im}^{\mathrm{T}}\mathbf{NCB}_{Jn}\mathrm{d}S + \int_{S_{u_I}} \mathbf{B}_{Im}^{\mathrm{T}}\mathbf{CN}^{\mathrm{T}}\mathbf{H}_{Jn}\mathrm{d}S \tag{19}$$

and

$$\mathbf{fU}_{Im} = \int_{S_{u_I}} \mathbf{B}_{Im}^{\mathrm{T}}\mathbf{CN}^{\mathrm{T}}\mathbf{u}^S \mathrm{d}S \tag{20}$$

with

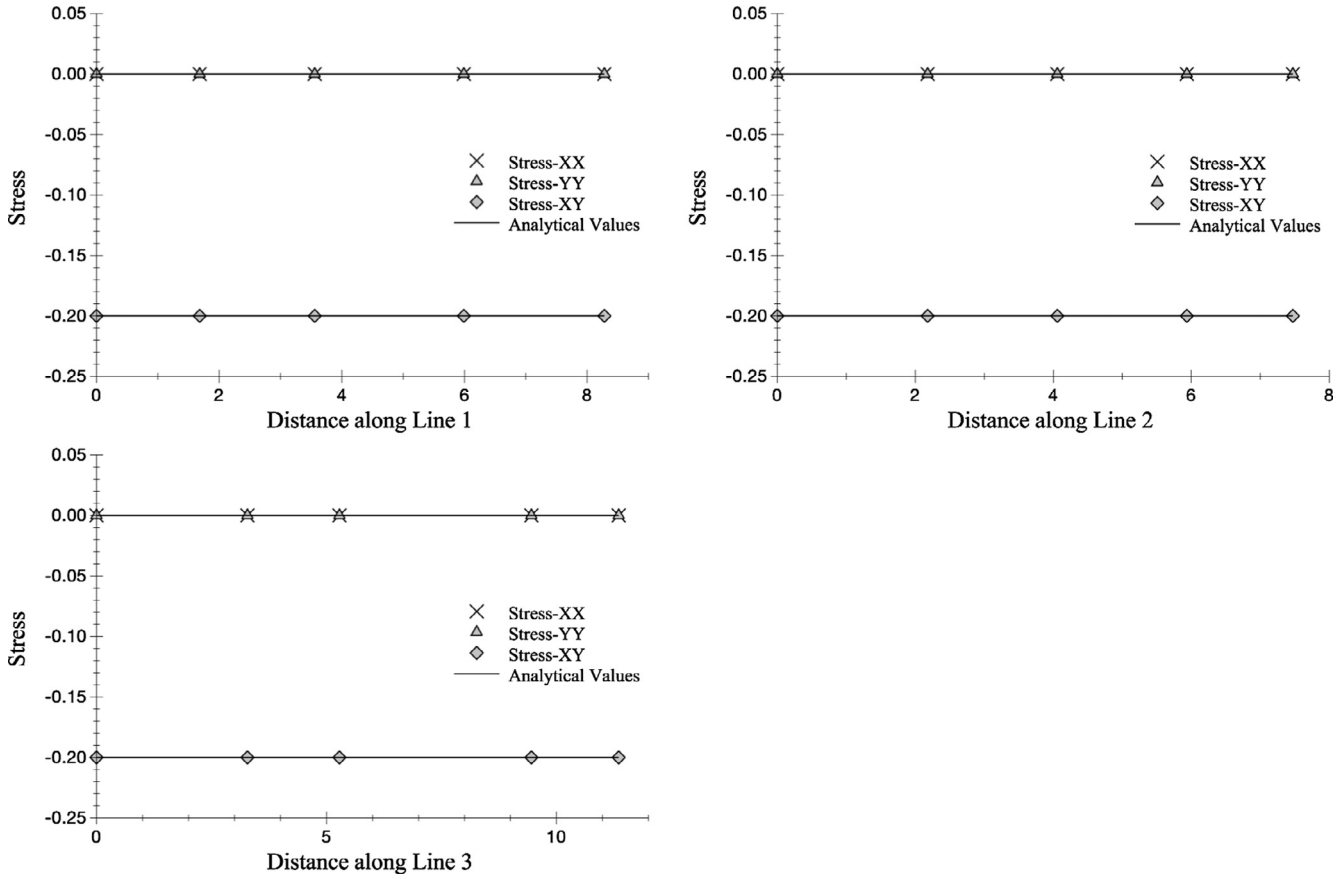

Fig. 10. Calculated stresses in the patch test study of Fig. 8 when constant shear stresses ($\tau_{xy} = -0.2$) are applied on the boundary.

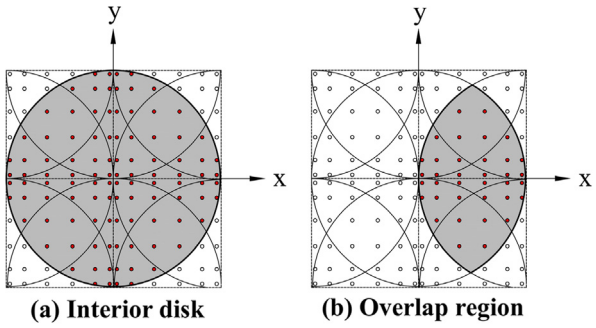

Fig. 11. Integration points for an overlapping disk element.

$$S_f = \bigcup_{I \in N_f} S_{f_I},\ N_f = \text{index set of nodes with nonzero intercept on the Neumann boundary}$$

and

$$S_u = \bigcup_{I \in N_u} S_{u_I},\ N_u = \text{index set of nodes with nonzero intercept on the Dirichlet boundary}$$

where **H** and **B** denote the displacement and strain interpolation matrices and the subscripts on **H** and **B** denote elements of these matrices.

We note that the boundary conditions are enforced using the expressions in Eq. (18). However, to impose the displacement boundary conditions we can also, in many cases, simply place the nodes of the overlapping elements along the boundary, and set the relevant degrees of freedom to the appropriate values in the solution vector.

3.2. Coupling with traditional finite elements

While the standard finite elements are formulated as given in many textbooks, see for example Ref. [1], the coupling of these elements with the overlapping elements is not standard. The interpolations need to be established to satisfy the rigid body mode conditions and the patch test, illustrated in Fig. 6. The displacement field of the coupling element in the subdomain $\Omega_{FE\text{-}FS}$ is given by the shape functions $h_I^{FE-FS}(\mathbf{x})$ and $h_{Jn}^{FE-FS}(\mathbf{x})$

$$\mathbf{u}_{\Omega_{FE-FS}}(\mathbf{x}) = \sum_{I \in \chi} h_I^{FE-FS}(\mathbf{x})(h_I \mathbf{u}_I + \sum_{\substack{K \in \kappa \\ K \neq I}} h_K \mathbf{a}_{K1}) + \sum_{J=1}^{nfs} \sum_{n \in \Im} h_{Jn}^{FE-FS}(\mathbf{x}) \mathbf{a}_{Jn} \tag{21}$$

where *nfs* is the number of overlapping elements which have an intersection with the coupling element, χ is the index set of the pure finite element nodes of the coupling element, κ is the index set of all the nodes of the coupling element, $\Im$ is the index set corresponding to the degrees of freedom of the Jth overlapping element that intersects the coupling element,

$$h_I^{FE-FS}(\mathbf{x}) = \frac{h_I(\mathbf{x})}{W} \tag{22}$$

$$h_{Jn}^{FE-FS}(\mathbf{x}) = \rho_J^{FE-FS}(\mathbf{x}) p_n(\mathbf{x}) \tag{23}$$

$$\rho_J^{FE-FS}(\mathbf{x}) = \frac{W_J(\mathbf{x})}{W} \tag{24}$$

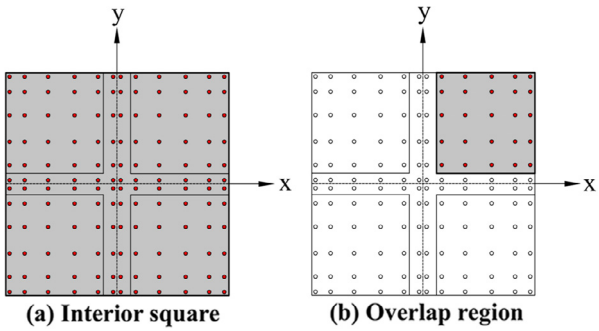

Fig. 12. Integration points for an overlapping quadrilateral element.

W is given by

$$W(\mathbf{x}) = \sum_{K=1}^{nfs} W_K(\mathbf{x}) + \sum_{I \in \chi} h_I(\mathbf{x}) \tag{25}$$

W_K is the weight function corresponding to the support of the overlapping element K, and h_I is the traditional interpolation function corresponding to the finite element node I. We use in Eq. (21) the unusual notation $\mathbf{a}_{K1}$ for the nodal degrees of freedom, these are equal to the $\mathbf{u}_K$.

Of course, the displacement interpolations used satisfy the partition of unity principle. Hence the rigid body modes can be represented.

With the above displacement interpolations, the relevant strain matrices and entries in the stiffness and mass matrices can be directly evaluated.

The patch test, see [1], for the new scheme is, as expected, passed since the interpolation functions have been constructed with that aim. Hence, the scheme satisfies the linear consistency property. For illustration, see Fig. 6, in conformance with our discussion in Section 2, the traditional finite elements are first generated, see Fig. 7(a). Then the overlapping elements are placed and extended to the finite element region Ω_{FE}, see Fig. 7(b). Finite element nodes located at the coupling boundary (where the finite

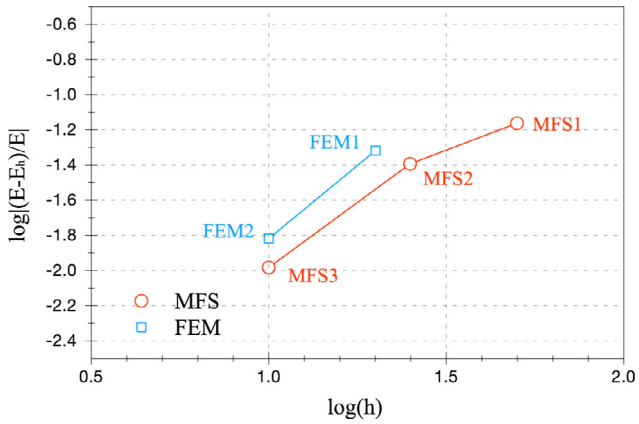

Fig. 15. Convergence of strain energy for the method of finite spheres and the finite element method.

Table 1
Strain energy errors and computational time multipliers of finite sphere discretizations as compared to the finite element reference solution.

Mesh	Number of nodes	Strain energy error (%)	Time multiplier
MFS1	80	6.87	0.68
MFS2	288	4.04	2.38
MFS3	3024	1.04	6.54

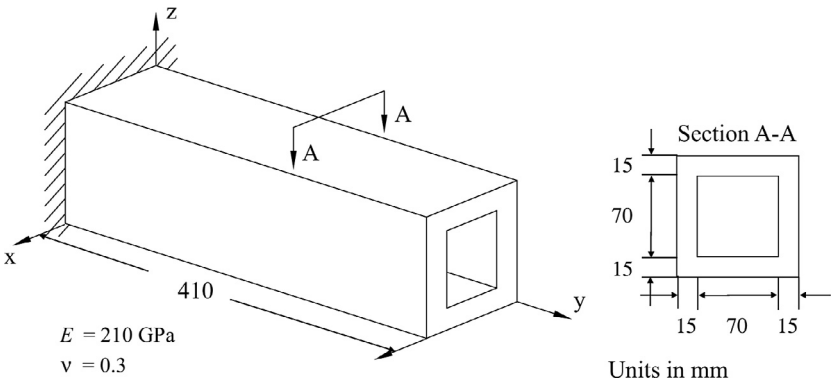

Fig. 13. Geometry, boundary conditions, and material data for short cantilever beam with square hollow section; the structure is loaded at its tip.

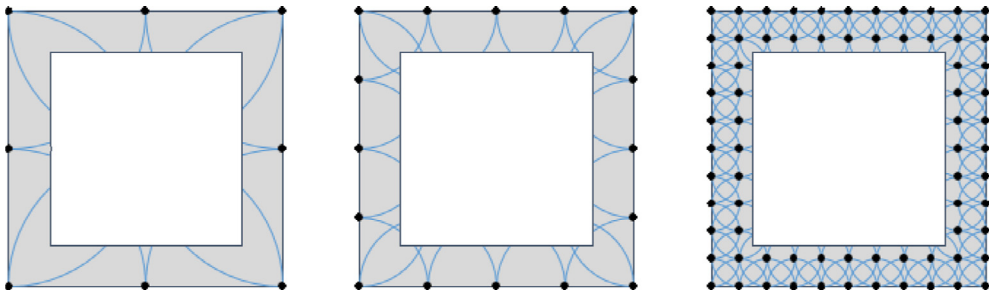

(a) MFS1: $r = 50$ mm (b) MFS2: $r = 25$ mm (c) MFS3: $r = 10$ mm

Fig. 14. MFS discretizations at Section A-A for short cantilever beam with square hollow section.

elements and overlapping elements intersect) are replaced with overlapping element nodes, see Fig. 7(c). Finally, finite elements adjacent to the coupling boundary become the coupling elements, see the green region $\Omega_{FE\text{-}FS}$ in Fig. 7(c). Hence, for Fig. 6, the index sets χ and κ used in Eq. (21) are, for the coupling element (shown in the figure), 1 and 1, 2, 3, 4, respectively.

Fig. 8 shows the "distorted patch" of elements also solved. First normal stresses are applied and then shear stresses are applied. Figs. 9 and 10 show the results.

3.3. Numerical evaluation of the element stiffness and mass matrices, load vectors

The stiffness and mass matrices and the load vector of the traditional elements are evaluated as usual, but special integration schemes are needed for the overlapping elements. Much effort has been spent in the development of meshless methods to obtain a reliable and efficient scheme. In a reliable scheme the integration ensures that the strain terms implicitly included in the interpolation are also contained in the numerically evaluated matrices and vectors. Unfortunately, for the overlapping elements (used here) a high order numerical integration is needed which is expensive.

We use for the overlapping elements a simple scheme based on standard Gauss numerical integration. The contributions from a 'quadrant' (or part thereof) pertaining to a sphere, square or overlap region are simply integrated with the commonly used Gauss integration schemes for quadrilateral domains. The contributions from Gauss points inside an overlapping finite element (or overlapping region) are added while all Gauss points outside the element (within or outside the analysis domain) are ignored. Figs. 11 and 12 illustrate schematically the numerical integration scheme for the overlapping spherical and quadrilateral elements. More details are given in Refs. [21,22]. The same approach is also used for the overlapping regions of these elements with traditional finite elements (the coupling elements).

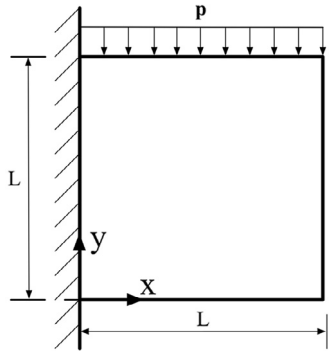

Fig. 16. A cantilever plate of unit thickness in plane strain conditions subjected to a uniformly distributed load, p = 1.0 per unit length (L = 2, E = 100, ν = 0.3).

3.4. Comments on the performance of overlapping finite elements

To give insight into the performance of the overlapping elements, we summarize here some important practical observations considering meshes in which *only* the spherical elements are used.

3.4.1. Static three-dimensional analyses

Some evaluations for two-dimensional solutions have been presented in Refs. [7,8,11,12,25,26], however a more severe evaluation is obtained in three-dimensional analyses. Such analyses are more complex and numerically more intensive, also in the required numerical integrations. Furthermore, static solutions provide a good evaluation because the stiffness matrix evaluation frequently corresponds to a large part of the solution effort. We quote here some solution results and comparisons from Ref. [22] in which for each analysis only a single load case is considered (which corresponds to a severe comparison). For this study the method was

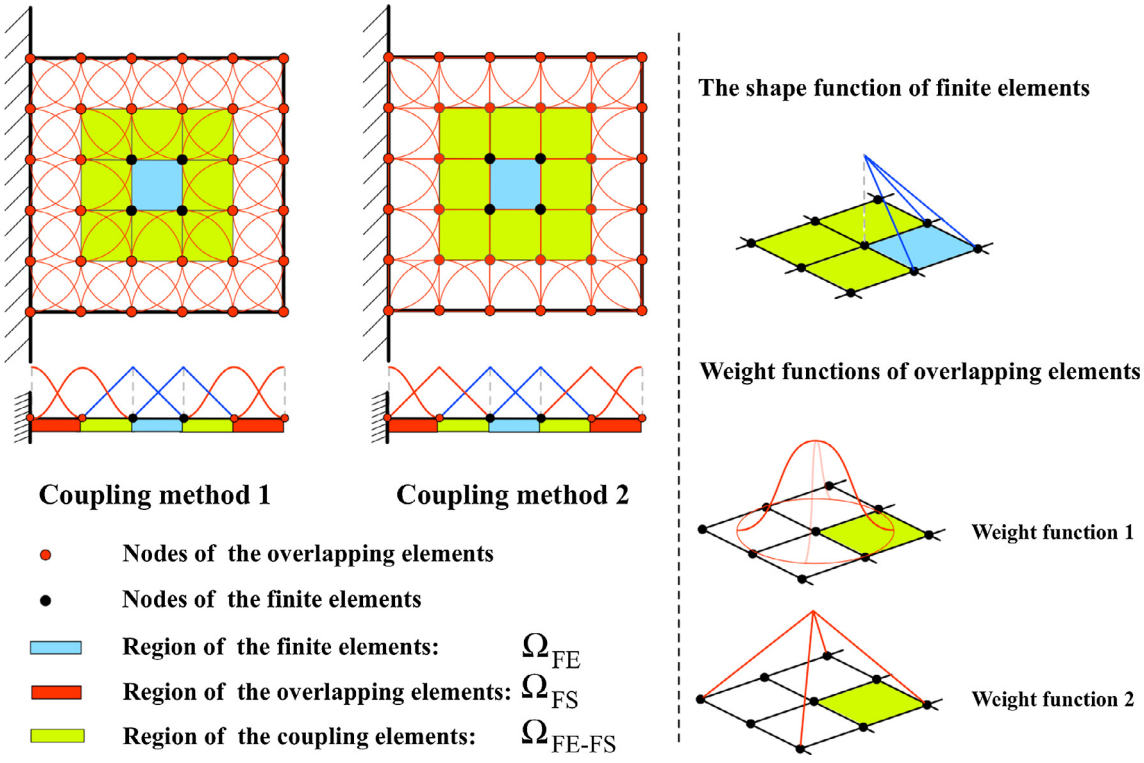

Fig. 17. Application of the coupling methods in the cantilever plate example.

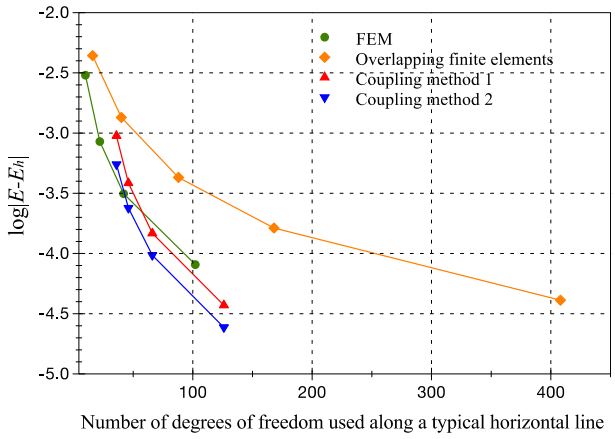

Fig. 18. Error as a function of the number of degrees of freedom. In each case the bilinear polynomial basis is used. The reference strain energy E of the cantilever plate is obtained using a 100×100 element mesh of 9-node finite elements.

implemented in the user-supplied element routine of ADINA in order to be able to use the same sparse solver for all analyses.

Fig. 13 shows the short cantilever beam of square hollow cross-section analyzed and Fig. 14 shows the finite sphere discretizations used. For spherical domains that are geometrically equal, the numerical integration is only performed once, and the result is then reused in the element assemblage process.

For the traditional finite element solutions, we use a sequence of compatible uniform meshes, uniformly refined, consisting of eight-node brick elements.

Fig. 15 gives the convergence of the solutions obtained and Table 1 gives some more details on these data. Here the error is calculated by comparison with the solution obtained using the finest traditional finite element mesh containing 32,400 nodes. This reference solution is deemed to be quite close to the unknown mathematically exact solution. The time multiplier gives how much faster (or slower) the solution is when compared to the reference solution.

For this analysis case, we see that if (about) a 1% error in strain energy is acceptable, using the overlapping spheres, the solution is about one order of magnitude more expensive. This conclusion becomes more favorable towards the finite sphere method when traditional 27-node brick elements are used. For more experiences see Ref. [22].

3.4.2. Dynamic analyses

Dynamic solutions are generally obtained using mode superposition or direct time integration. Both solution approaches can be effective depending on the problem solved.

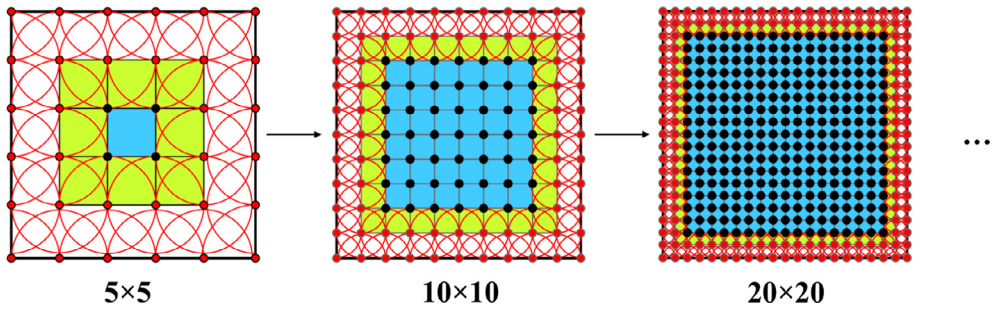

Fig. 19. Schematic of h-type uniform refinement used. During the mesh refinement, always only two layers of overlapping elements are at the domain boundary.

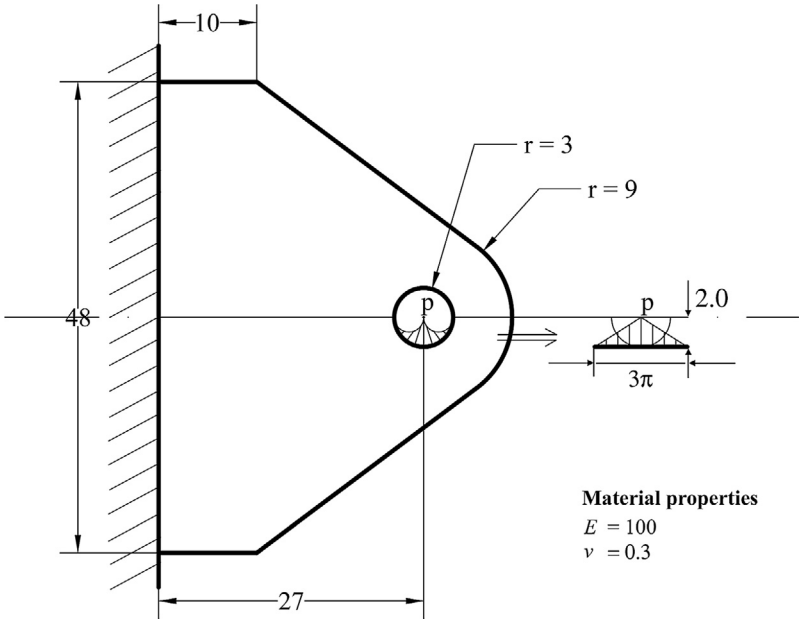

Fig. 20. Geometry of bracket as obtained from the CAD program.

In direct time integration, the Newmark method trapezoidal rule is widely employed but the implicit Bathe method can be more effective because it provides more accurate solutions. Both schemes do not use any integration parameters to be adjusted [1,27].

An analysis field in which accurate solutions are difficult to obtain is the field of wave propagations. In traditional finite element analyses, the waves are difficult to compute accurately because an optimal time step has to be selected, and this step depends on the speed of the wave [1,28]. If the time step is larger than the optimal time step, the solution is unstable when using conditionally stable schemes (e.g. the central difference method) and loses accuracy when using unconditionally stable schemes (e.g. the trapezoidal rule). Moreover, in all time integrations using traditional finite element discretizations, if a time step *smaller* than the optimal time step is used, the solution accuracy is *worse*. In practical analyses, multiple waves (e.g. compression, shear and Rayleigh waves) might be propagating at different speeds of which only one can be chosen for the optimal time step selection. Therefore, the other waves will not be accurately solved for.

Table 2
Analysis of the bracket example: comparison of the total number of degrees of freedom (DOF) and calculated strain energy $E_{h.}$

Meshing scheme	DOF	Strain energy
The finite element method	16,862	1.07
The new meshing scheme	1884	1.02

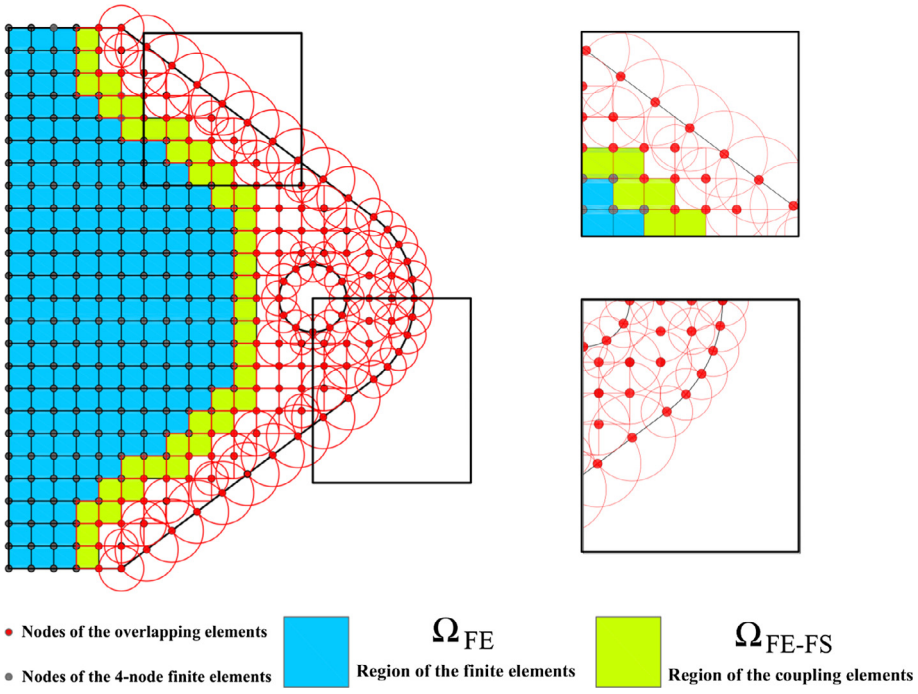

Fig. 21. The mesh of the new scheme in the analysis of the bracket.

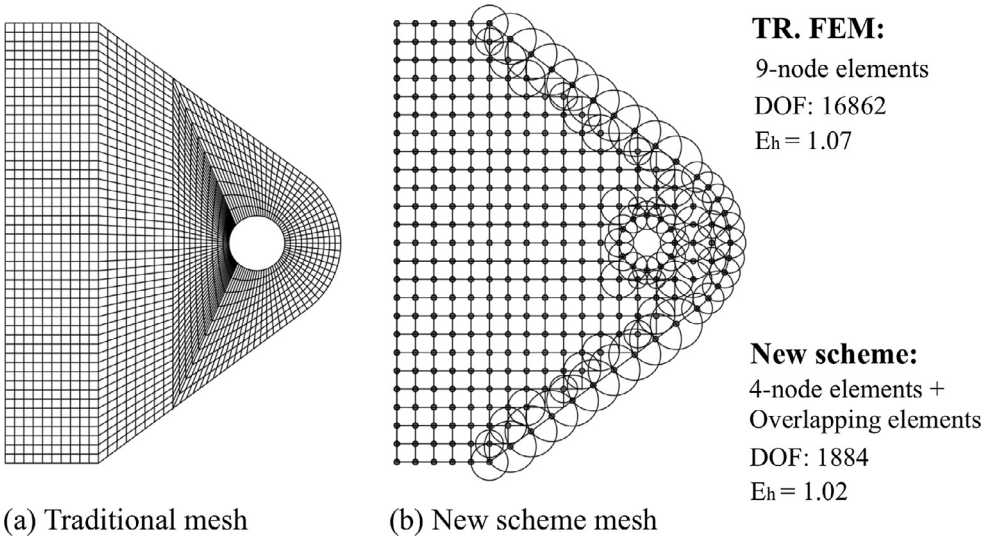

Fig. 22. The meshes used.

An important observation using the method of finite spheres with harmonic functions is that a *decrease* in the time step size leads to an *increase* in solution accuracy, shown for the Bathe implicit time integration scheme in Ref. [21]. This is an important fact and is what an analyst intuitively would like to see. With this characteristic, in practical analyses, the largest wave speed can be chosen to establish the time step size, with the other waves then automatically being solved for more accurately.

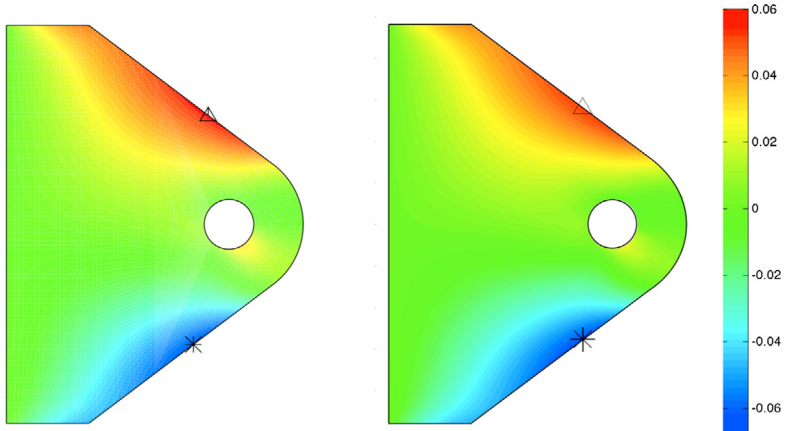

(a) Displacement u (left: ADINA; right: new scheme)

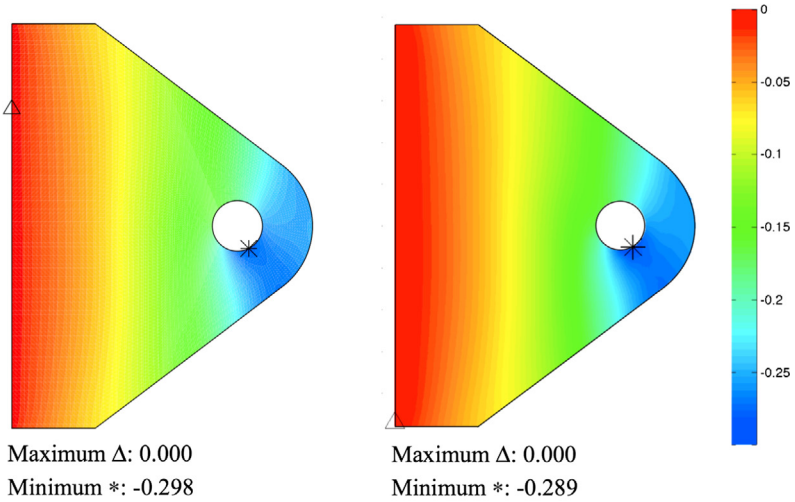

(b) Displacement v (left: ADINA; right: new scheme)

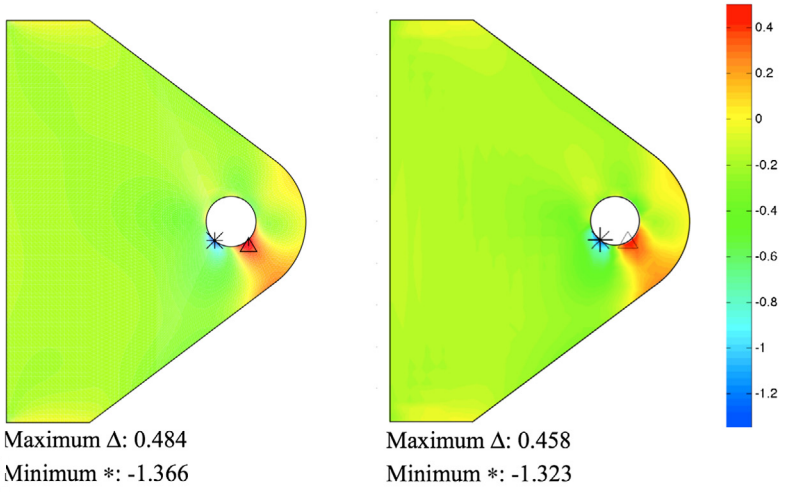

(c) Stress τ_{xy} (left: ADINA; right: new scheme)

Fig. 23. Some solution results in the analysis of the bracket.

The details of mathematical analysis are given in Refs. [21,23] where also solutions are shown to illustrate this important fact regarding the selection of the time step size. These solutions also show that in some analyses the use of the overlapping finite elements is quite effective when compared to the use of traditional finite elements.

The other approach widely used for dynamic analyses, but largely for structural response solutions, is mode superposition [1]. In the traditional finite element discretizations, by far, the largest solution effort is in calculating the required frequencies and mode shapes. Considering the overlapping elements, we can conjecture that the approach may be competitive compared to the use of traditional finite elements because less degrees of freedom may be used in the method of finite spheres and the major solution effort will also be in solving the eigenvalue problem, and not in establishing the **K** and **M** matrices. However, actual numerical comparisons should be established.

4. Illustrative solutions

In this section, we present two numerical examples to show the application of the new meshing scheme. In the first example, a cantilever plate problem is solved, the solution convergence of the new scheme is studied and compared with results using the traditional finite element method and the method of finite spheres. In the second example, a bracket problem is considered. The use of the new coupling scheme is discussed, and numerical results are presented and compared.

While the solution with the new scheme uses mostly still considerably more computational time than the traditional approach, we do not yet give relative solution times, because we want to focus in this paper only on generically presenting the new scheme. More research and development is needed to reach an implementation as effective as possible of the new meshing and solution scheme before an assessment of effort is appropriate.

4.1. A cantilever plate under a uniformly distributed load

In the first example, we consider a cantilever plate in plane strain conditions subjected to a uniformly distributed load (see Fig. 16). The solution domain is decomposed into three regions (see Fig. 17): the regions of finite elements Ω_{FE}, overlapping elements Ω_{FS}, and coupling elements $\Omega_{FE\text{-}FS}$. In this example, two coupling methods are investigated. In the "coupling method 1", the quartic spline weight function (weight function 1, see Fig. 17), is chosen for the overlapping elements at the coupling boundary. In the "coupling method 2", the hat function is used as the weight function (weight function 2, see Fig. 17).

Fig. 18 shows the convergence of the strain energy when h-type uniform refinement is performed (see Fig. 19). The meshes using the overlapping elements only near the plate boundary give the best results when measured in terms of the number of degrees of freedom used. The reason is that the boundary stresses can be most effectively (in terms of degrees of freedom) captured in this way.

4.2. Analysis of a bracket problem with the new meshing scheme

The new meshing scheme is employed to analyze a bracket with unit thickness in plane stress conditions, see Fig. 20. The bracket problem is first analyzed with the traditional finite element method meshed with 9-node elements. The resulting strain energy $E_h = 1.07$.

The mesh used in the new scheme is shown in Fig. 21. Four-node finite elements are used. We note that some cells internal to the CAD geometry have not been converted to 4-node elements but are covered by overlapping elements. These all use the quadratic basis in Eq. (7). Since the solution of the cantilever plate problem showed that the numerical results are more accurate when the hat function is used as the weight function in the coupling, we use this coupling procedure in the analysis of the bracket.

Table 2 compares the total number of degrees of freedom (DOF) and calculated strain energy using the new meshing scheme and the traditional finite element method, for which the solution was obtained with a very fine mesh of 9-node elements using ADINA. Fig. 23 gives some fields of solution results.

5. Concluding remarks

The objective in this paper was to present a new meshing and analysis scheme for CAD driven finite element simulations.

We presented a meshing scheme which is directly operating on CAD geometries. The scheme gives undistorted traditional finite elements (like rectangles in two-dimensional simulations) in the interior of the geometries and uses overlapping finite elements near the boundaries of the CAD part. This meshing procedure is easy to use and computationally effective.

We summarized the theoretical formulation of the overlapping finite elements including the coupling to traditional finite elements. In comments on the performance of the overlapping elements when used to discretize the complete analysis domain, we focused on the use of the spherical elements (used in the method of finite spheres). While showing good attributes, in static and dynamic analyses, the overlapping elements are mostly still computationally expensive when used to discretize a *complete* geometric domain.

However, the use of the new meshing scheme with overlapping finite elements shows much promise. We presented some illustrative solutions in which the meshing operates directly on the CAD part, and the numerical simulation is obtained with little human effort. This feature of small human effort in the new paradigm to obtain CAD driven numerical simulations renders the new analysis approach very attractive.

As in almost all new developments, there are, however, a number of modeling and analysis features in the proposed scheme that need more research, like, to render the new meshing scheme of the CAD geometries fully automatic including the automatic elimination of geometry defects, to establish the accuracy obtained in static and dynamic solutions for different meshes, to reach more effective spatial numerical integration schemes, to develop the complete scheme for application to shell structures, and of course to reach the effective solution of complex nonlinear and multiphysics problems. We have so far focused on increasing the efficiency of the scheme for the linear analysis of solids, see Ref. [29].

References

[1] Bathe KJ. Finite element procedures. Prentice Hall; 1996. 2nd ed. KJ Bathe, Watertown, MA; 2014.
[2] Sedeh RS, Pan K, Adendorff MR, Hallatschek O, Bathe KJ, Bathe M. Computing nonequilibrium conformational dynamics of structured nucleic acid assemblies. J Chem Theory Comput 2015;12:261–73.
[3] Nayroles B, Touzot G, Villon P. Generalizing the finite element method: diffuse approximation and diffuse elements. Comput Mech 1992;10:307–18.
[4] Belytschko T, Krongauz Y, Organ D, Fleming M, Krysl P. Meshless methods: an overview and recent developments. Comput Meth Appl Mech Eng 1996;139:3–47.
[5] Duarte CA, Oden JT. An h-p adaptive method using clouds. Comput Method Appl Mech Eng 1996;139:237–62.
[6] Atluri SN, Zhu T. A new meshless local Petrov-Galerkin (MLPG) approach in computational mechanics. Comput Mech 1998;22:117–27.
[7] De S, Bathe KJ. The method of finite spheres. Comput Mech 2000;25:329–45.
[8] De S, Bathe KJ. Displacement/pressure mixed interpolation in the method of finite spheres. Int J Numer Meth Eng 2001;51:275–92.
[9] Liu GR. Meshfree methods: moving beyond the finite element method. Taylor & Francis; 2009.

[10] Dolbow J, Belytschko T. Numerical integration of the Galerkin weak form in meshfree methods. Comput Mech 1999;23:219–30.
[11] De S, Bathe KJ. The method of finite spheres with improved numerical integration. Comput Struct 2001;79:2183–96.
[12] De S, Bathe KJ. Towards an efficient meshless computational technique: the method of finite spheres. Eng Comput 2001;18:170–92.
[13] Mazzia A, Ferronato M, Pini G, Gambolati G. A comparison of numerical integration rules for the meshless local Petrov-Galerkin method. Numer Algorithms 2007;45:61–74.
[14] Babuška I, Banerjee U, Osborn JE, Li Q. Quadrature for meshless methods. Int J Numer Meth Eng 2008;76:1434–70.
[15] Babuška I, Banerjee U, Osborn JE, Zhang Q. Effect of numerical integration on meshless methods. Comput Mech Appl Mech Eng 2009;198:2886–97.
[16] Starius G. Composite mesh difference methods for elliptic boundary value problems. Numer Math 1977;28:243–58.
[17] Steger JL, Benek JA. On the use of composite grid schemes in computational aerodynamics. Comput Mech Appl Mech Eng 1987;64:301–20.
[18] Chesshire G, Henshaw WD. Composite overlapping meshes for the solution of partial differential equations. JCP 1990;90:1–64.
[19] Henshaw WD, Petersson NA. A split-step scheme for the incompressible Navier-Stokes equations. Numer Simul Incompressible Flows 2003;2502:108–25.
[20] Henshaw WD. A high-order accurate parallel solver for Maxwell's equations on overlapping grids. SIAM J Sci Comput 2006;28:1730–65.
[21] Ham S, Lai B, Bathe KJ. The method of finite spheres for wave propagation problems. Comput Struct 2014;142:1–14.
[22] Lai B, Bathe KJ. The method of finite spheres in three-dimensional linear static analysis. Comput Struct 2016;173:161–73.
[23] Kim KT, Bathe KJ. Transient implicit wave propagation dynamics with the method of finite spheres. Comput Struct 2016;173:50–60.
[24] Bathe KJ. The finite element method with 'overlapping finite elements'. In: Zingoni A, editor. Proceedings Sixth International Conference on Structural Engineering, Mechanics and Computation – SEMC 2016, Cape Town, South Africa.
[25] Hong JW, Bathe KJ. Coupling and enrichment schemes for finite element and finite sphere discretizations. Comput Struct 2005;83:1386–95.
[26] Macri M, De S. Towards an automatic discretization scheme for the method of finite spheres and its coupling with the finite element method. Comput Struct 2005;83:1429–47.
[27] Bathe KJ, Noh G. Insight into an implicit time integration scheme for structural dynamics. Comput Struct 2012;98–99:1–6.
[28] Noh G, Ham S, Bathe KJ. Performance of an implicit time integration scheme in the analysis of wave propagations. Comput Struct 2013;123:93–105.
[29] Zhang L, Bathe KJ. Overlapping finite elements for a new paradigm of solution (in preparation).